FACTA UNIVERSITATIS
Series: **Working and Living Environmental Protection** Vol. 21, Nº 4, Special Issue, 2024, pp. 271 - 282
https://doi.org/10.22190/FUWLEP241003026J

Original scientific paper

MULTI-SLOPE ENERGY DECAY CURVES GENERATED BY MOVING AVERAGE APPROACH

UDC 543.843.7

Marko Janković[1], Dejan Ćirić[1], Maro Puljizević[2], Aleksandar Pantić[3]

[1]University of Niš, Faculty of Electronic Engineering in Niš, Serbia
[2]Knauf Insulation d.o.o., Škofja Loka, Slovenia
[3]Knauf Insulation d.o.o., Surdulica, Serbia

ORCID iDs:	Marko Janković	https://orcid.org/0009-0002-1109-3241
	Dejan Ćirić	https://orcid.org/0000-0003-4974-3131
	Maro Puljizević	N/A
	Aleksandar Pantić	https://orcid.org/0000-0003-2351-498X

Abstract. *Sound energy decay is typically represented by an energy decay curve (EDC), which depicts the decrease in sound energy over time after the sound source in a room is turned off. In spaces with single-slope decay, the EDC appears as a straight line. Such curves can be analyzed using linear regression to calculate parameters such as reverberation time. However, due to factors like room geometry, absorption, and other effects of sound transmission in enclosed spaces, an EDC may exhibit multi-slope decay. When linear regression is applied to such a curve, the results depend heavily on the range over which the curve is approximated by a straight line.*
This paper analyzes EDCs generated using the moving average approach, based on impulse responses measured in two rooms: a reverberation chamber and a classroom. The focus is on multi-slope EDCs and a comparison between moving average EDCs and those generated using the Schroeder backward integration method. The moving average EDCs exhibit a greater dynamic range than the Schroeder-integrated EDCs, revealing the final part of the reverberation decay, which is obscured in the latter due to the cumulative summation of background noise.

Key words: *sound energy decay, energy decay curve, moving average, multi-slope decay*

1. INTRODUCTION

Sound energy decay is a very important characteristic in room acoustics, particularly in performance spaces like auditoria [1,2]. The concept of energy decay refers to the gradual reduction in sound as it dissipates over time after the sound source has stopped due to

Received October 3, 2024 / Accepted November 21, 2024
Corresponding author: Dejan Ćirić
University of Niš, Faculty of Electronic Engineering in Niš, Aleksandra Medvedeva 4, 18000 Niš, Serbia
E-mail: dejan.ciric@elfak.ni.ac.rs

factors such as absorption, reflection, diffusion and other acoustic interactions [2-5]. This phenomenon is crucial in the study of room reverberation. Reverberation time (RT), a key parameter for room acoustics, describes the time required for the sound pressure level in a room to decrease by 60 dB once the sound source is turned off [2-4].

The sound decay is typically represented by energy decay curves (EDCs) or functions, which are important for understanding how sound behaves in rooms. In the sound decay process, acoustic conditions can be assumed to be static, but also dynamic where factors like room geometry or the position of sound sources vary [3]. Numerous studies address the challenge of estimating sound decay, particularly RT calculated from the EDC. Understanding the decay of sound energy is essential for assessing the acoustical properties of spaces, like clarity of sound in rooms such as classrooms or concert halls [4].

EDCs can be generated in different ways. One of the traditional methods includes the measurement of a room impulse response (RIR) and backward integration of this RIR, introduced by Schroeder [6,7]. Here, the squared RIR is integrated over reverse time to produce the EDC. The generated EDC shows a continuous decline as energy is absorbed by the room's materials and dissipated into the air. By plotting the EDC on a logarithmic scale, the sound decay becomes evident, where an exponential decay typically appears as a straight line. The Schroeder integration allows for detailed EDC analysis. It represents an important instrumental in identifying how sound diminishes over time in a given environment, especially in spaces with complex acoustical properties [1,8], such as capturing the multiple sloped decays [9]. One of the main benefits of the Schroeder integration is its ability to smooth out fluctuations in the decay, providing a clearer view of the reverberation process. However, the method has some drawbacks, particularly its sensitivity to background noise. The cumulative summing of noise in real-world RIRs can distort the EDC, causing the late decay part of the curve to bend upwards, which compromises the accuracy of the RT measurements [10]. In this way, a useful dynamic range of such an EDC is reduced.

From the implementation point of view, linear fitting of the reverberation decay of Schroeder decay curves is often applied, which might lead to inaccurate results in practice [1]. This is why a number of references deal with proposals on how to overcome this situation, e.g., improve the procedures of calculating the quantities from the EDCs as RT and absorption coefficient [11]. Going in that direction, some proper parametric models are proposed in the literature, as done in [1], allowing for a better understanding of energy decay, thereby enabling more effective acoustic design and analysis of rooms like auditoria.

In contrast to ideal conditions where the reverberation decay of an EDC should form a straight line on a logarithmic plot, in real-world settings, deviations are common, leading to multi-slope or concave shapes [12]. In rooms with uneven absorption, the EDC can display complex behaviors, especially at low frequencies, such as double-slope decay, where the initial decay is faster than the subsequent decay. When analyzing these deviations**,** the use of linear regression to estimate the slope (calculate RT) requires careful selection of the dynamic range – range where this regression is applied. The wider the dynamic range, the more likely it is that deviations from the ideal linear decay will affect the estimated slope. Therefore, the focus of this study is on multi-slope EDCs measured in a reverberation chamber.

This paper presents an alternative method for generating EDCs by applying a moving average to the logarithm of squared RIRs. The proposed approach is compared with the traditional method, which is based on Schroeder's backward integration of squared RIRs.

The focus is on multi-slope EDCS and their analysis for the purpose of calculating relevant quantities from EDCs, such as reverberation time. The potential of the proposed moving average approach is demonstrated through characteristic examples of EDCs from different environments. For this purpose, both synthesized and measured RIRs are used.

2. Multi-slope Decays and Linear Regression

2.1. Single-Slope versus Multi-Slope Decays

Multi-slope energy decays are common in various environments, such as coupled spaces, rooms with non-uniform distributions of absorbing materials and reverberation chambers [7,11]. In these cases, the energy decay exhibits multiple slopes, indicating different decay rates at various stages of the sound's dissipation [8]. Multi-exponential decays are influenced by factors such as room shape, scattering objects, and absorber positioning. For example, in rectangular rooms, non-grazing modes decay faster, contributing to the curvature of the energy decay [9]. The literature highlights that a uniform distribution of absorptive materials leads to more consistent and reliable EDCs [13]. Additionally, seating positions in a room can affect the sound energy decay pattern, too [6]. In seats near lateral walls, energy decay plateaus are observed due to early reflections, while seats in the middle display a more stable, exponential decay.

EDCs in non-diffuse environments also deviate from the standard exponential decay typically seen in diffuse sound fields [14]. In such environments, non-diffuse fields can accelerate energy decay due to the formation of the anisotropic sound field. When analyzing the EDC and calculating RT, non-diffuse sound decay is critical, as the non-linearity of the EDC can result in inconsistent RT values across different measurement intervals [14,15]. The presence of multi-exponential decay (i.e., decay curve non-linearity) complicates RT calculation in EDC analysis.

In spaces with multi-slope EDCs, the sound decay cannot be modeled by a single exponential function. Instead, an approach is to use multi-exponential decay functions, which incorporate multiple exponential terms to represent the different rates at which sound decays [7,16]. Research of EDC in reverberation chamber utilizes the exponential fits rather than traditional linear regression methods, highlighting that multi-exponential decays more accurately reflect the complex acoustic conditions present [9]. While this approach is useful, it can become overly complex, especially when applied to environments with spatially varying source-receiver configurations or non-uniform absorption properties [16]. A contrasting approach would be to use a "common-slope model," which simplifies the analysis of reverberation by describing sound energy decay with a set of common decay rates or slopes, regardless of spatial and directional variations [16].

2.2. Approaches to Solve Linear Regression Problem

The decay functions generated by the Schroeder backward integration are a valuable tool for distinguishing between single-slope and multiple-slope decay characteristics. However, challenges arise when utilizing these functions. One challenge relates to deviations from expected exponential decay patterns caused by noise, as highlighted in [1]. Another issue, mentioned in a number of references, is the use of linear regression (or the single-exponential decay model) to calculate the slope of the Schroeder EDC, specifically

the reverberation decay [17]. This approach is often insufficient for environments with complex acoustic properties. As a result, it is suggested that a more accurate framework beyond traditional linear regression is required [11]. In other words, more advanced modeling techniques are needed to better capture the complexity of the decay process.

As a result, advanced methods such as nonlinear regressions, Bayesian analysis, and artificial neural networks (NNs) have been developed to improve the accuracy of sound decay analyses [1]. For instance, nonlinear regression is applied in [6] to determine the early time limit in EDCs. Identifying this early time limit, which separates direct sound from lateral reverberation, enhances the accuracy of distinguishing early reflections from late reverberation. Additionally, a nonlinear decay model, incorporating a double-slope decay term and noise, is also applied to detect the truncation time of an RIR used in EDC generation through Schroeder integration [15].

A Bayesian decay time estimation framework is introduced in [11] as an alternative to traditional methods. This framework allows for more accurate modeling of the initial energy decay, which is often discarded in linear regression approaches. By focusing on this initial portion, the framework provides more reliable estimates of decay times, even in cases of multi-exponential decays. Three methodologies — the variable projection algorithm (VARPRO), regularized inverse Laplace transform (RILT), and maximum entropy decay-time distribution (MEDD) — are introduced in [17] to achieve more robust, accurate, and time-efficient analysis, particularly when multiple decay slopes are present. Each of these methodologies is designed to handle complex EDCs.

Another approach involves the use of deep NN for estimating the decay slope, or more specifically, the RT under both static or dynamic conditions [3]. In a recent study, NNs are used to estimate the parameters of multi-slope EDCs, including the decay rates and amplitude of each exponential component [7]. Another NN-based method models multi-slope decays, where the network estimates key parameters such as decay times and amplitudes for different slopes [18].

3. METHODOLOGY

3.1. EDC Generated by Moving Average

To address the limitations of Schroeder integration, an alternative approach based on averaging the logarithmic squared RIR (applying the moving average) has been explored in [10]. In this approach, a decay curve is first generated by taking the logarithm of the squared RIR, resulting in a curve with strong fluctuations. Then, each point on this curve is replaced by the average value of the data points within a window of a certain length, with the point to be replaced positioned at the center of the window. This process is repeated along the entire logarithmic squared RIR curve, from beginning to end. This is why the described procedure is referred to as the moving average.

The moving average method reduces fluctuations and provides a smoother EDC. It is particularly advantageous in noisy environments where traditional methods might be skewed. Unlike the Schroeder method, this approach does not involve cumulative summing, thus eliminating noise-related distortion. As a result, a greater dynamic range of the EDC is obtained compared to the Schroeder method. However, it also presents challenges, particularly in selecting the appropriate averaging interval (the size of the averaging window) that must be carefully chosen. A window that is too short may not

sufficiently smooth the fluctuations, while a larger window can introduce distortions, especially at the beginning of the curve or near the "knee" – the intersection between reverberation decay and noise floor [10].

It is shown in [10] that the best results are typically obtained when the averaging window contains around 5000 data points (with a sampling frequency of 44.1 kHz). This provides a balance between reducing fluctuations and maintaining accuracy. The optimal window size varies depending on the frequency band, with higher frequencies requiring shorter windows. Additionally, the exact window length depends on the specific characteristics of the RIR. While averaging helps mitigate noise effects, it is not without drawbacks. For example, the averaging process can distort the initial part of the EDC, especially when the window is too large.

In this study, both the Schroeder integration and moving average method are used to generate the EDCs, see Fig. 1. These curves are compared in terms of their shape and dynamic range, which represents the range of decay from the beginning of the curve up to a certain point, such as the knee of the curve.

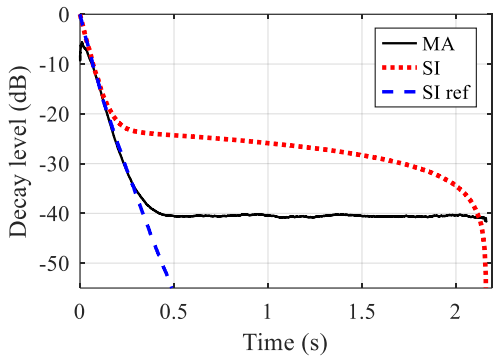

Fig. 1 EDCs generated from noisy synthesized RIR by moving average (MA) and Schroeder integration (SI) together with EDC generated by Schroeder integration from noiseless synthesized RIR (SI ref)

3.2. RIRs used for generating EDCs

Two types of RIRs are used for this study: synthesized and measured. The synthesized RIRs are generated using the image source model, as described in [19], resulting in noiseless RIRs. Depending on the model parameters, these RIRs can exhibit varying degrees of irregularities, such as curvatures in the reverberation decay. In order to have noisy RIRs, white or pink noise of a particular amplitude (level) is added. The sampling frequency for these RIRs is set to 44.1 kHz.

The measured RIRs were obtained from two different rooms: a reverberation room and a classroom, having RT from 6 s to 11 s and from 1.6 s to 1.9 s at mid frequencies, respectively. Both rooms are located at the Faculty of Electronic Engineering in Niš. The construction elements of the reverberation room are typical for such spaces, as shown in Fig. 2.a), featuring an irregular shape and ceiling-mounted diffusers. A unique feature of this room is its small volume, only 65.05 m^3, which is below the volume specified in the ISO 354 standard for sound absorption measurement. Generally, it is assumed that a diffuse

sound field is generated in a reverberation room, where sound decay should be truly exponential, represented by a single slope. However, numerous studies have shown that this assumption does not always hold in practice, especially when absorption materials are unevenly distributed within the room [20]. The second room used for measurements is a typical classroom, with unique ceiling geometry, as shown in Fig. 2.b). The floor area of this room is approximately 117 m^2, with a ceiling height of about 2.8 m at the lower section and around 4 m at the higher section. As with the synthesized RIRs, the sampling frequency for the RIRs measured in both rooms was 44.1 kHz.

Fig. 2 Rooms where RIRs were measured: a) reverberation room, and b) classroom

4. Analysis of Generated EDCs

One of the major challenges in generating EDCs using the moving average approach is selecting the appropriate window size for averaging the data points (averaging interval). The window size must be chosen as a compromise to produce a sufficiently smooth EDC without losing important details from short decays. The effects of varying the window size in generating broadband EDC are presented in Fig. 3.

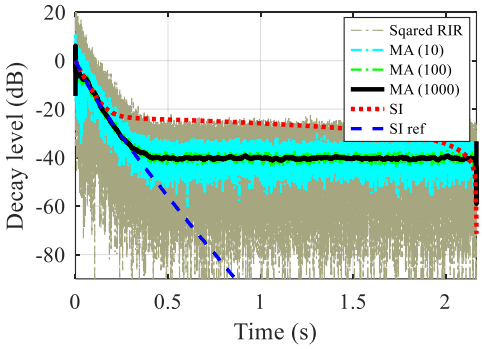

Fig. 3 EDCs generated from noisy synthesized RIR by moving average (MA) and Schroeder integration (SI) using different averaging intervals (given in number of samples in legend) together with EDC generated by Schroeder integration from noiseless synthesized RIR (SI ref)

Since the moving average approach does not involve the cumulative summing of noise, it results in a greater dynamic range of the EDC compared to Schroeder backward integration, as shown in Fig. 4. A longer averaging window smooths out fluctuations caused by both noise and the reverberation process, At the same time, the slope of the EDC remains largely unchanged (close to that of the reference EDC – noiseless Schroeder EDC), except when the averaging window is too long, as seen in Fig. 4.

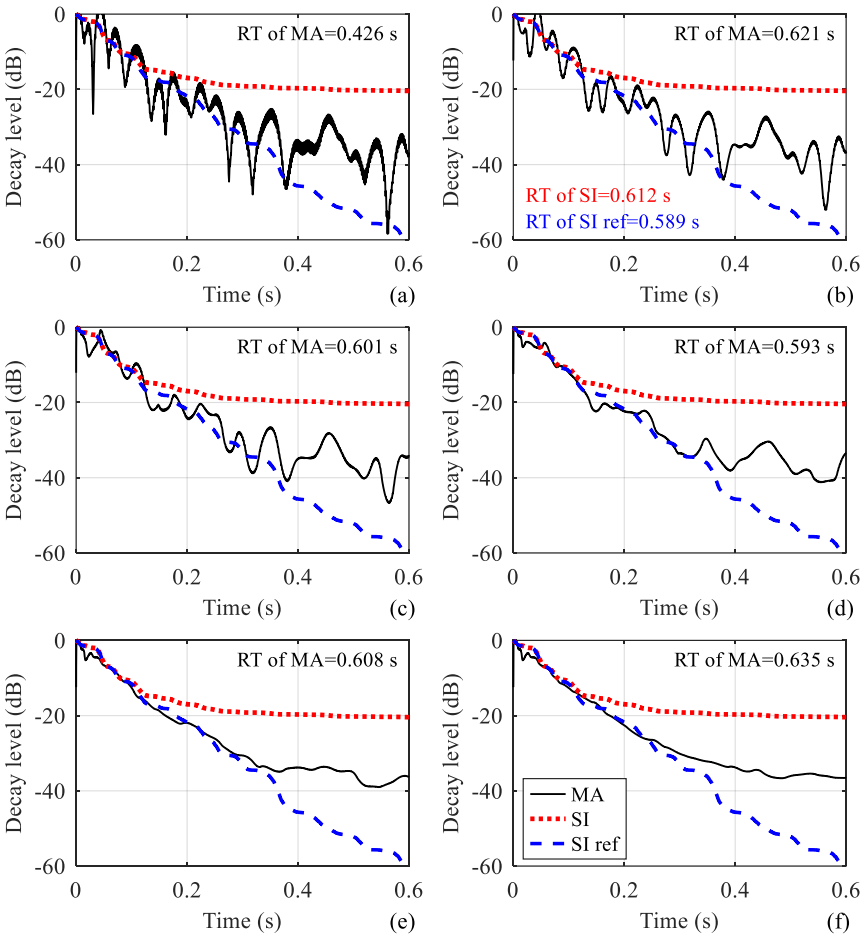

Fig. 4 EDCs generated from noisy synthesized RIR by moving average (MA) using different averaging window sizes: a) 100, b) 500, c) 1000, d) 2000, e) 5000 and f) 10000 samples, together with EDCs generated by Schroeder integration (SI) from both noisy and noiseless synthesized RIR (SI ref)

To illustrate the use of these curves, the RT is calculated by applying linear regression within the same range (the decay range between -5 dB and -30 dB) from both the moving average EDCs and reference (noiseless Schroeder) EDC. The RT is also calculated in the same manner from the noisy Schroeder EDC, but using the decay range from -5 dB to -

15 dB, since the available dynamic range of this curve is too small. From the calculated RTs, shown in Fig. 4, it is evident that a short averaging interval in the moving average method may lead to a significant deviation of the obtained RT from the reference one of the noiseless EDC. This deviation decreases as the averaging interval increases, and for a window size of 200 samples already, the relative error of RT in comparison to the reference RT is reduced to about 5%, see Fig. 4.b). Further increasing the averaging interval results in a smoother EDC, but the calculated RT remains almost unchanged, see Fig. 4.c) to 4. e). However, an overly long averaging interval can alter the global shape of EDC, including its slope, and the calculated RT, see Fig. 4.f).

The dynamic range of the noisy Schroeder EDC used for RT calculation is significantly smaller than that of the moving average EDC (in this case, too small), and the calculated RT differs from the reference RT for a certain amount. This difference strongly depends on the EDC shape and the dynamic range used for regression. The effect of the applied dynamic range is less significant or even negligible in single-slope, flat EDCs, but this is not the case in Fig. 4.

Analyzing an EDC and calculating parameters such as RT becomes more complex when the EDC exhibits multi-slope decay. Such EDCs used for calculating absorption coefficient are investigated in [12]. When generating multi-slope EDCs using the moving average approach, the choice of averaging window size becomes even more critical. The reverberation decay of a multi-slope EDC can be divided into multiple segments, each with its own slope. In this case, the averaging interval for points near the boundary between segments will include data from both segments, each with different slopes. As a result, the EDC shape may change, especially near these segment boundaries, and this effect is more pronounced with longer averaging intervals.

At the same time, if an appropriate averaging window size is used to generate the EDC, the curve will exhibit a larger dynamic range, as mentioned earlier, and it will reveal parts of the sound decay that are not visible in the Schroeder EDC. This is illustrated in Fig. 5, which presents multi-slope and concave-shaped EDCs generated from the RIRs measured in the reverberation room. While the multi-slope nature is less visible in some of the curves, such as in Fig. 5.b) and d), which show a concave reverberation decay, the double-slope decay becomes more prominent in the moving average EDCs.

The effects of changing the averaging interval when generating a multi-slope EDC from the RIR measured in the reverberation room are shown in Fig. 6, presenting the curves generated from the same RIR as in Fig. 5.c). The general characteristics of the moving average EDC are visible in all curves, regardless of the averaging interval, including the greater dynamic range compared to the Schroeder EDC and the double-slope decay. As the averaging interval increases, the distant features of the reverberation decay become more prominent. EDC irregularities, such as fluctuations and curvatures, are typically more pronounced in the third-octave bands at lower frequencies, as shown in Figs. 5 and 6.

When comparing the moving average and Schroeder EDCs for RT calculation, the most significant difference lies in the dynamic range available for this calculation. This is especially important for methods like linear regression. The mentioned difference is illustrated in Fig. 7, which shows double-slope EDCs in the third-octave band at 200 Hz generated from the RIR measured in the reverberation room. Linear regression is applied to two different regression ranges corresponding to two different slopes. While the range is the same for the first slope, it is considerably larger for the moving average approach in the case of the second slope.

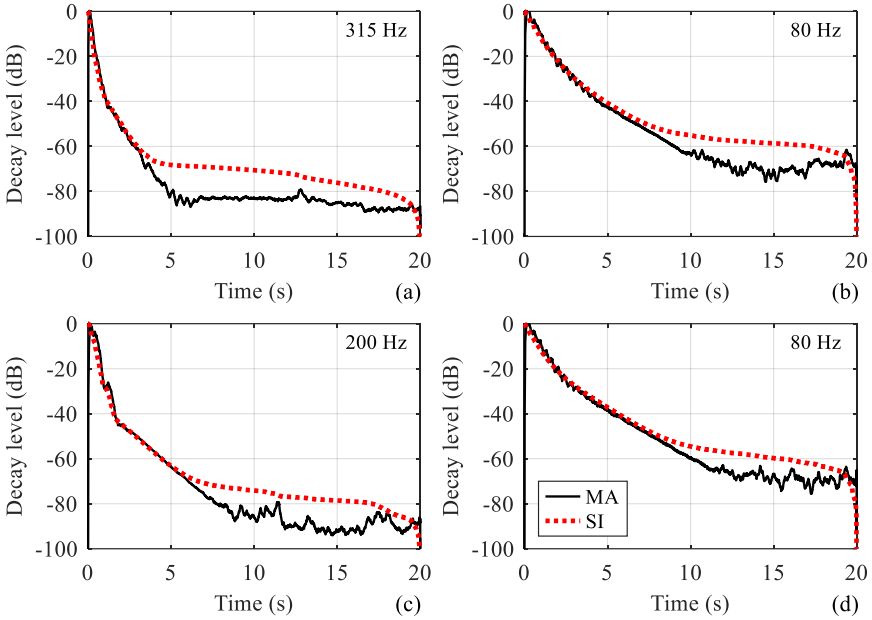

Fig. 5 EDCs in third-octave bands generated from RIRs measured in reverberation room by moving average (MA) (averaging in 10000 samples) and Schroeder integration (SI)

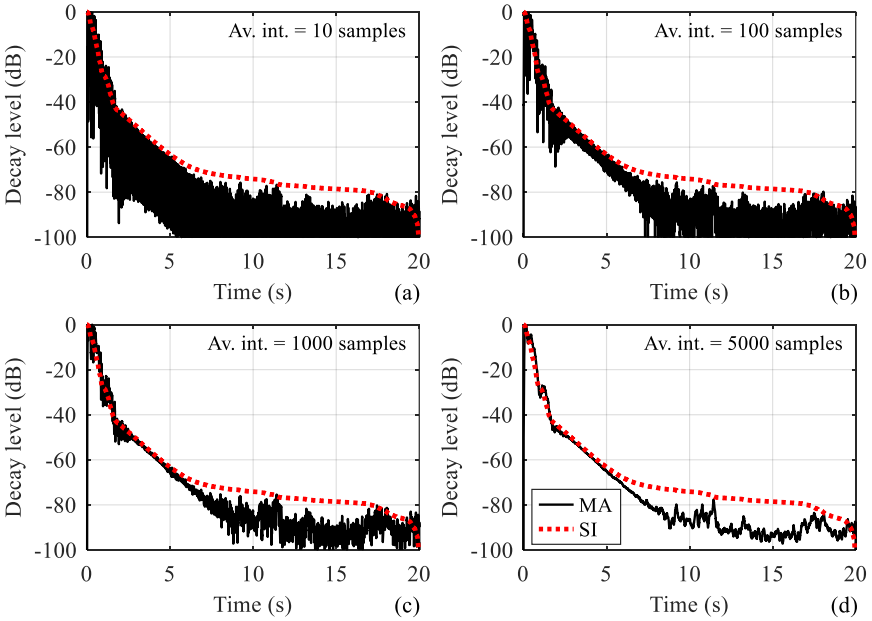

Fig. 6 EDCs in third-octave band at 200 Hz generated from RIR measured in reverberation room by moving average (MA) (different averaging intervals) and Schroeder integration (SI)

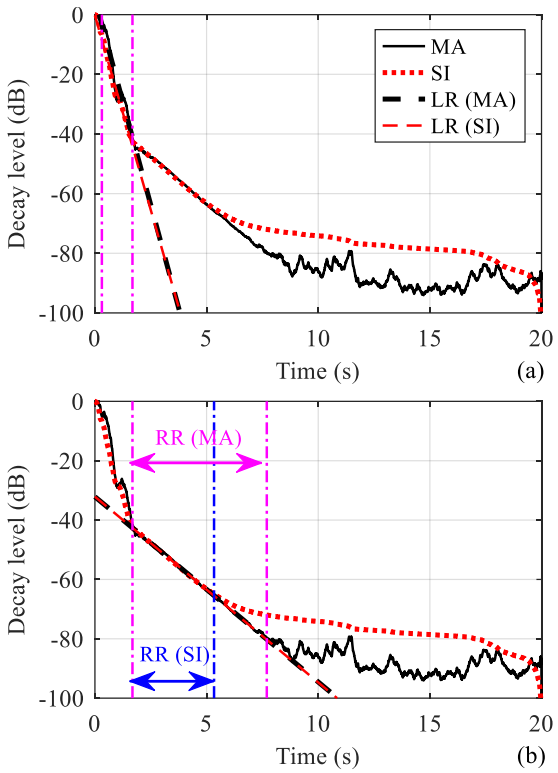

Fig. 7 EDCs in the third-octave band at 200 Hz generated from RIR measured in reverberation room by moving average (MA) (averaging in 10000 samples) and Schroeder integration (SI), as well as linear regression (LR) lines for both methods (MA and SI) and a) the first slope, and b) the second slope (RR = regression range)

The RIRs measured in the second room (the classroom) are mainly regular, and this is also reflected in the EDCs generated from these RIRs, as shown in Fig. 8. Although a slightly concave shape is observed in the EDC in the third-octave band at 100 Hz, the EDCs are primarily single-slope decay curves. Some fluctuations in the reverberation decay can be seen, particularly at low frequencies, as shown in Fig. 8.b). The EDCs obtained by the moving average and Schroeder integration methods coincide well up to the point near the knee of the Schroeder EDCs. Beyond that point, the moving average EDCs typically continue to descend by about 15 dB or more dB, depending on the characteristics of the RIRs.

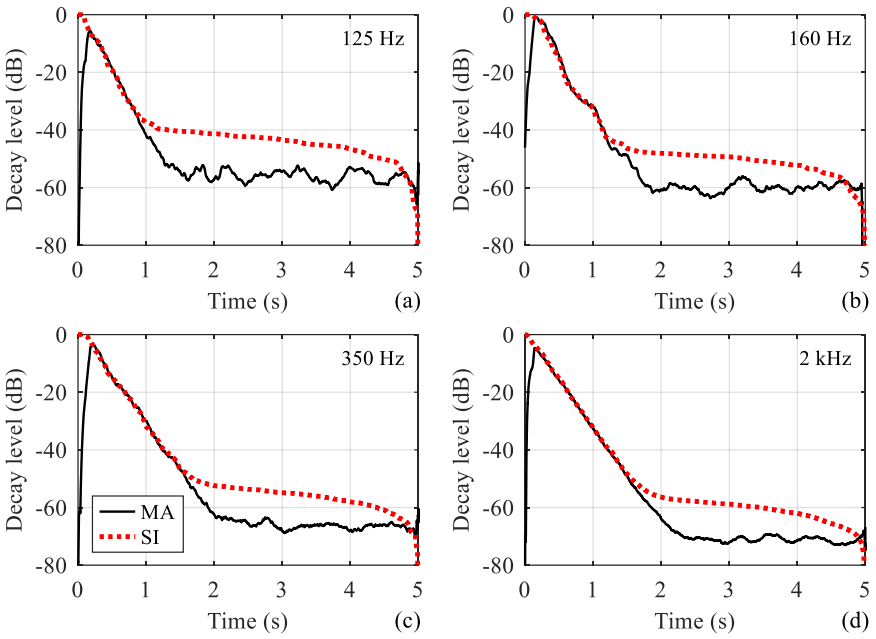

Fig. 8 EDCs in third-octave bands generated from RIRs measured in the classroom by moving average (MA) (averaging in 10000 samples) and Schroeder integration (SI)

5. Conclusions

The study presents a comprehensive comparison between the moving average approach and Schroeder integration for generating EDCs, emphasizing the benefits and limitations of each method. The moving average method offers significant advantages, particularly in environments with noise, as it avoids the cumulative summing process used in Schroeder integration, which can distort the later parts of the decay curve. By averaging the logarithmic squared RIRs, the moving average method produces smoother curves, reducing fluctuations and improving the dynamic range of the EDC. This extended dynamic range allows for better detection of the final stages of reverberation decay, which are often obscured in traditional methods due to noise interference.

However, in the moving average method, if the averaging window is too short, it may fail to sufficiently smooth fluctuations, while a window that is too long can introduce distortions, especially at critical points like the start of the curve or near the "knee," where the reverberation decay transitions into the noise floor. Despite this challenge, when the window size is carefully chosen, the method not only provides a clearer representation of sound decay but also allows for more accurate RT calculations, particularly in complex acoustic environments where multi-slope decays are present. The study demonstrates that the moving average method is a robust alternative, offering improved accuracy for analyzing acoustic spaces with complex or multi-slope energy decay patterns.

Acknowledgement: *This work was supported by the Ministry of Science, Technological Development and Innovation of the Republic of Serbia [grant number 451-03-65/2024-03/200102].*

REFERENCES

1. Xiang N., Gul Z. Su, (2023), Efficiency of sound energy decay analysis in auditoria, *Auditorium Acoustics 2023*, Athens, Greece, September 28-30, 2023, DOI:10.25144/16006.
2. Muhammad N. I., Abdullahi M. Y., Aliyu A. B., (2023), Comparison of blind reverberation time estimation in an enclosed space by analysing energy decay curve, *Fudma Journal of Sciences*, Vol. 7, No. 3, 2023, pp. 194-200, DOI:10.33003/fjs-2023-0703-1762.
3. Götz P., Tuna C., Walther A., Habets E. A. P., (2022), Blind reverberation time estimation in dynamic acoustic conditions, *ICASSP 2022 - 2022 IEEE International Conference on Acoustics, Speech and Signal Processing (ICASSP)*, Singapore, Singapore, May 22-27, 2022, pp. 581-585, DOI:10.1109/ICASSP43922.2022.9746457.
4. Nowoświat A., (2023), Determination of the reverberation time using the measurement of sound decay curves, *Applied Science*, Vol. 13, 2023 p. 8607, DOI:10.3390/app1315860.
5. Kanev N., (2011), Sound decay in a rectangular room with specular and diffuse reflecting surfaces, *Forum Acusticum 2011*, Aalborg, Denmark, June 27-July 1, 2011, pp. 1935-1940.
6. Xia C. Q., Tang S. K. (2023), Finding early time limits t_e with nonlinear regression on energy decay curves, *Auditorium Acoustics 2023*, Athens, Greece, September 28-30, 2023.
7. Götz, G., Hold, C., McKenzie, T., Schlecht, S., Pulkki, V., (2022), Analysis of multi-exponential and anisotropic sound energy decay, *Jahrestagung für Akustik – DAGA 2022*, Stuttgart, Germany, March 21-24, 2022.
8. Edwards N., Kemp J. A., Gül Z. S., (2022), Measurement and subjective responses to the sound decay from coupled volumes in the McPherson Room, St Andrews University, *24th International Conference on Acoustics*, Gyeongju, Korea, October 24-28, 2022.
9. Balint J., Muralter F., Nolan M., Jeong C.-Ho, (2018), Energy decay curves in reverberation chambers and the influence of scattering objects on the absorption coefficient of a sample, *Euronoise 2018*, Crete, Greece, May 27-31, 2018, pp. 2025-2030.
10. Miletić M., Ćirić D., Janković M., (2019), Usage of averaging in generation of room energy decay curve, *International Conference on Electrical, Electronic, and Computing Engineering (IcETRAN)*, Srebrno Jezero, Serbia, June 3-6, 2019, pp. 29-34.
11. Balint J., (2020), *Evaluating the Decay of Sound*, Ph.D. Thesis, Graz University of Technology, Austria, 2020.
12. Ćirić D., Puljizević M., Pantić A., Janković M., (2024), Effects of energy decay curve deviation on absorption coefficient calculation, *59th International Scientific Conference on Information, Communication and Energy Systems and Technologies (ICEST)*, Sozopol, Bulgaria, July 1-3, 2024.
13. Wogu G. C., (2017), *Reverberation Time Analysis Averaged by Energy Decay Curve*, M.Sc. Thesis, Thesis, London South Bank University, UK, 2017.
14. Novoselova A., Kanev N., (2020), Decay of non-diffuse sound fields in a room, *MATEC Web of Conferences*, September 24, 2020, Article number 00006.
15. Chen M., Lee C.-M., (2022), The optimal determination of the truncation time of non-exponential sound decays. *Buildings*, Vol. 12, 2022, p. 697, DOI:10.3390/buildings12050697.
16. Götz G., Schlecht S. J., Pulkki V., (2023), Common-slope modeling of late reverberation, *IEEE/ACM Transactions on Audio, Speech, and Language Processing*, Vol. 31, 2023, pp. 3945-3957, DOI:10.1109/TASLP.2023.3317572.
17. Muralter F., Balint J., (2019), Analysis tools for multiexponential energy decay curves in room acoustics, *Jahrestagung für Akustik – DAGA 2019*, Rostock, Germany, March 18-21, 2019, pp. 1302-1305.
18. Götz G., Falcon Perez R., Schlecht S., Pulkki, V., (2022), Neural network for multi-exponential sound energy decay analysis, *Journal of the Acoustical Society of America*, Vol. 152, No. 7, 2022, pp. 942-953, DOI:10.1121/10.0013416.
19. Lehmann E. A., Johansson A. M., (2008), Prediction of energy decay in room impulse responses simulated with an image-source model, *Journal of the Acoustical Society of America*, Vol. 124, No. 1, 2008, pp. 269-277, DOI:10.1121/1.2936367.
20. Balint J., Berzborn M., Nolan M., Vorländer M., (2023), Measuring sound absorption: The hundred-year debate on the reverberation chamber method, *Acoustics Today*, Vol. 19, No. 3, 2023, pp. 13-21, DOI:10.1121/AT.2023.19.3.13.